Bistable State Switch Enables Ultrasensitive Feedback Control in Heterogeneous Microbial Populations

Xinying Ren [1,*], Christian Cuba Samaniego[2,*], Richard M. Murray[1], and Elisa Franco [2]

***Abstract*— Ultrasensitive feedback control can improve robust gene expressions in cell populations, yet it usually requires large chemical productions that cause severe burden to cells. Inspired by 'division-of-labor' in heterogeneous populations, we propose a bistable switch circuit that utilizes quorum sensing systems to coordinate heterogeneous phenotypes' behaviors. We show that ultrasensitivity emerges from a collection of parallel bistable switches in individual cells. When applied to feedback control of population level expressions, it can achieve robust reference tracking and adaptation to disturbances. In particular, we demonstrate that molecular sequestration enables tunable hysteresis in single switches, leading to a wide range of stable population level expressions.**

I. Introduction

Advances in synthetic biology improves our ability to engineer genetic circuits and build microbes with controllable and complex functionalities. Desired functionalities such as biochemical synthesis, toxin degradation and drug delivery, often depend on population level expressions [1], [2], [3]. It is important for an engineered microbe to exhibit robust population expressions to fulfill functionalities in fluctuating environments, also known as adaptation to disturbances [4]. Tunable expressions are also needed when the functionality requires accurate and tight regulations, such as balancing metabolic fluxes in biochemical production and controlling drug dosage [5], [6].

In previous studies, circuits have been studied and designed at single cell level to achieve robust and tunable gene expressions in homogeneous cell populations [7], [8], [9], [10]. Ultrasensitive feedback control has been proposed to improve robust expressions by amplifying the error in the output due to the disturbance and providing a high gain feedback [11], [12]. Yet ultrasensitive controllers are not easy to implement with synthetic circuits in cells. Such high gains are often realized by transcription and translation of a large amount of proteins, causing a strong burden to the host cell [13]. Therefore, implementable ultrasensitive controllers may require new circuit structures without relying on large productions.

Engineering ultrasensitive control circuits can be challenging at single cell level in homogeneous cell populations. However, there is a huge potential to design implementable control circuits at population level when cells exhibit heterogeneous states. Heterogeneity in gene expressions is common in natural microbial populations and often leads to phenotypes with diverse behaviors [14]. Heterogeneous populations are observed to better adapt to environmental disturbances through cellular state switching [15], [16]. Moreover, heterogeneity in expressions is considered as a strategy of 'division-of-labor' to relieve burden in single cells [17].

In heterogenous populations, state switching at single cell level can generate a sharp change in ratios between phenotypes at population level. It suggests that the ultrasensitivity can emerge in heterogeneous populations and can be harnessed in population level feedback control. In this paper, we explore design principles and circuit implementations that realize ultrasensitive feedback control in heterogeneous populations. We start with a bistable switch circuit at single cell level and demonstrate a positive feedback loop with molecular sequestration generates tunable hysteresis. Then we present how ultrasensitivity is generated at population level by multiple switches in parallel. Finally, we show the bistable switch circuit mediated by quorum sensing signals enables robust reference tracking and adaptation to disturbances in the closed loop.

For the rest of the paper, we will consider capital letter for chemical species, and lower case letter for its corresponding concentration. For example, species X has concentration x.

II. Ultrasensitive Feedback Control Improves Robustness in Population Expressions

A. Ultrasensitive Feedback Control

In dynamical systems, ultrasensitive feedback can be used to attenuate error in the output caused by unknown disturbances. With an ultrasensitive feedback controller, the closed-loop system is expected to robustly track a reference and reject disturbances in the process dynamics.

Fig. 1A shows a general closed-loop diagram of a feedback controller and a process. The output Y of the process is the input to the controller, and the controller produces U as an output to actuate the process as an input. Therefore, the steady state of the closed loop is determined by the intersection of input-output mappings of the controller and the process. When the controller is ultrasensitive, the input-output map of the controller exhibits a sharp transition, as demonstrated in Fig. 1A, right panel. Input-output maps of the controller (orange line) and the process (black line) intersect at the equilibrium of the closed-loop system. As long as the equilibrium is stable and lies in the ultrasensitve regime, the output Y defined by the intersection always converges to the threshold of the sharp transition, even when the process is uncertain or perturbed by disturbances

* Equal contribution [1]Department of Control and Dynamical Systems, California Institute of Technology, California 91125, USA. xrren@caltech.edu [2]Department of Mechanical and Aerospace Engineering, University of California Los Angeles, California 90095, USA. ccubasam@g.ucla.edu,efranco@seas.ucla.edu

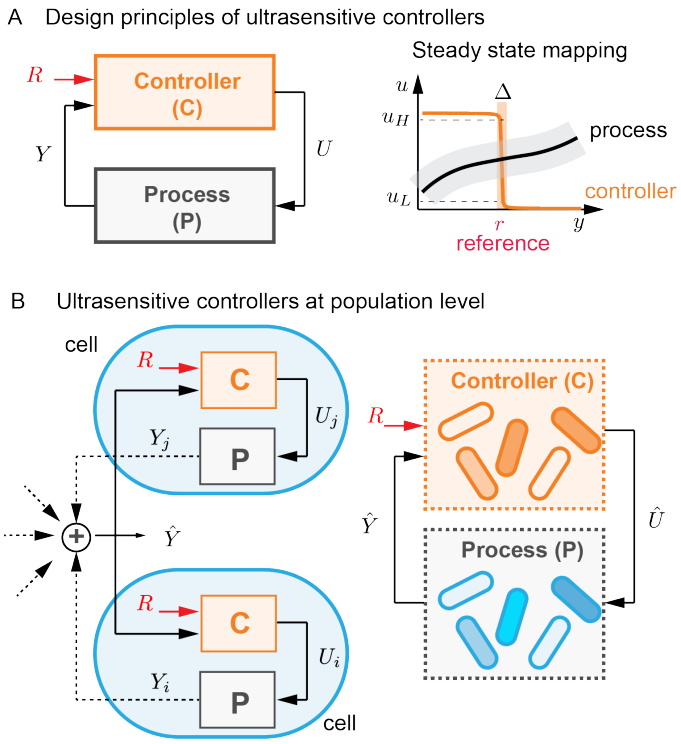

Fig. 1. **Ultrasensitive feedback controllers** Panel A presents a closed-loop diagram with an ultrasensitive feedback controller. The steady state input-output mapping demonstrates that the output is determined by the intersection of input-output maps and converges to the reference. Panel B is a schematic figure of a controlled system of a cell populations. The process in each cell is regulated by the same control circuit while the output is the total of cells' outputs. The population level process can be considered under the regulation of a population level controller with an overall $\hat{U}$ and $\hat{Y}$.

(gray area). Our ability to tune the threshold externally is analogous to setting the reference.

In synthetic biology, the controller and the process often refer to regulated gene expressions by biomolecular reactions. Implementing ultrasensitive feedback control using molecular reactions faces some challenges. Simple networks such as molecular sequestration or phosphorylation requires large production rates to deliver an ultrasensitive response [12], [18], [19]. Large production of chemicals may induce burden to cells, which can become detrimental. Therefore, we need to figure out implementable ultrasensitive controllers without relying on large production rates in single cells.

B. Ultrasensitive Controllers At Population Level

In many synthetic biology applications, required functionalities of microbial cells are evaluated at population level. If synthetic circuits are directly designed at population level, we might be able to avoid constraints at single cell level, such as large production rates required for ultrasensitive controllers.

We consider a genetically-identical cell population of n cells. The control objective is the population level expression of a target species $\hat{Y}$. Assume the i-th cell produces the target species at a concentration y_i. The population level expression is considered as the sum of all single cells' expressions, so

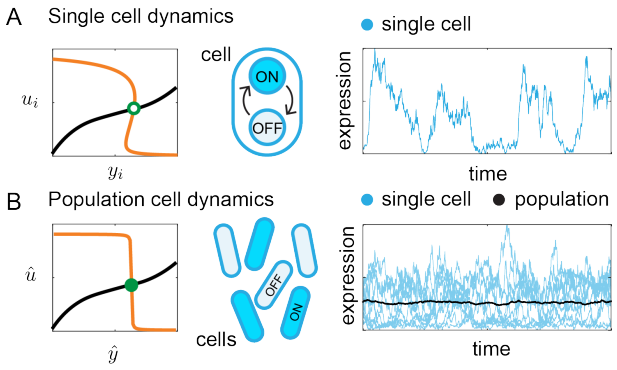

Fig. 2. **Ultrasensitive responses of bistable switches** Panel A shows the steady state input-output mapping of a single bistable switch and its dynamics. A bistable switch has two stable states (ON and OFF) and an unstable intermediate state. The intersection of input-output maps of the process and the single bistable switch results in an unstable equilibrium (empty green dot), and the stochastic trajectory of the single cell shows frequent state transitions. Panel B illustrates the population level response and dynamics of multiple bistable switches. The steady state input-output mapping shows a stable equilibrium (filled green dot). The trajectory of population expression exhibits a constant output (black line).

we have the concentration of $\hat{Y}$ as

$$\hat{y} = \sum_{i=1}^{n} y_i. \tag{1}$$

We assume all cells are under regulation of an identical synthetic circuit with feedback control, as shown in Fig. 1B, left panel. These controllers actuate cells' outputs Y_i by inputs U_i, and cooperatively drive the population level output $\hat{Y}$ to a reference R.

To perform population level design of control circuits, we first define the population level process and controller, as shown in Fig. 1B, right panel. Although physical implementations of circuits are based on biomolecular reactions inside each cell, the control mechanisms are better understood using a population level description. The population level process is defined as the sum of single cells' processes, and is actuated by an overall control input $\hat{U}$ and produces $\hat{Y}$. The population level controller takes $\hat{Y}$ as an input and compares it with the reference R and generates $\hat{U}$ in output.

An ultrasensitive controller requires an ultrasensitive input-output response. We notice that a bistable switch circuit enables ON and OFF states with different gene expressions in a single cell, as shown in Fig. 2A. The hysteresis can generate a sharp switch in its input-output mapping. However, when combining a bistable switch with the process, the input-output maps' intersection falls in the neighborhood of unstable equilibrium, leading to local instability in the closed loop, as shown in Fig. 2A, left panel. In addition, stochasticity of the cellular environment also causes a bistable switch to exhibit frequent state switching behaviors, as illustrated in Fig. 2A, right panel. Therefore, the bistable switch does not operate as a stabilizing ultrasensitive feedback controller in single cells.

On the other hand, if there are multiple bistable switches in parallel, we propose that it is possible to stabilize the

total output by exploiting the sum of heterogeneous states of individual cells, as shown in Fig. 2B. The population operates as multiple single cells in parallel, thus bistable switches in individual cells can be considered as parallel switches. Moreover, the stochastic state switching behaviors in single cells do not interfere with the stable population level expressions, as shown in Fig. 2B, right panel. With this approach, bistable switch circuits can be used as an ultrasensitive controller at population level.

In addition to the ultrasensitive response in the controller, it is necessary to design a sensor of the total output to coordinate switches in individual cells in a closed-loop system. We suggest that quorum sensing signals can be used to close the loop between the population level process and controller. Quorum sensing molecules can be secreted, diffuse and mix in environments to form a global signal and activate downstream gene expressions in cells. Therefore, quorum sensing systems have been widely used in engineered microbial consortia to facilitate cell-cell collaborations [20].

III. Sequestration Generates Tunable Hysteresis In A Bistable Switch

We first build a bistable switch circuit that exhibits hysteresis in a single cell. A bistable switch in synthetic biology usually requires a positive feedback loop with high cooperativity. Recent studies have shown that sequestration with positive feedback is also sufficient to generate bistability [21]. In the following subsections, we consider a bistable switch circuit including a positive feedback and sequestration as an example.

A. A Single Bistable Switch With Molecular Sequestration

We present a circuit design including a self-activating species X_i, sequestered by a species Z_i, as shown in Fig. 3A. We assume the self-activation kinetics follows a Hill-type function, and production, degradation and sequestration follow the law of mass action. We can write down the model:

$$\dot{x}_i = \alpha + \theta\frac{x_i}{x_i + K} - \delta x_i - \gamma x_i z_i \quad (2)$$

$$\dot{z}_i = \beta - \delta z_i - \gamma x_i z_i. \quad (3)$$

The production rates α and β can be varied by external inputs, for example with inducible promoters.

We consider α and β as inputs to the bistable switch. When α is the input, we call it the activator mode, since the input activates X_i production. On the other hand, the inhibitor mode corresponds to β being the input and inhibiting X_i through sequestration. The output of the bistable switch should actuate the target expression when it is applied as the controller to the process. We assume such actuation is based on a Hill-type activation by X_i, so we define the output of the bistable switch U_i:

$$u_i = \frac{x_i}{x_i + K}. \quad (4)$$

Now, we test if the bistable switch has an ultrasensitive response. We derive closed-form solutions from a third order equilibrium equation that depends on parameters presented

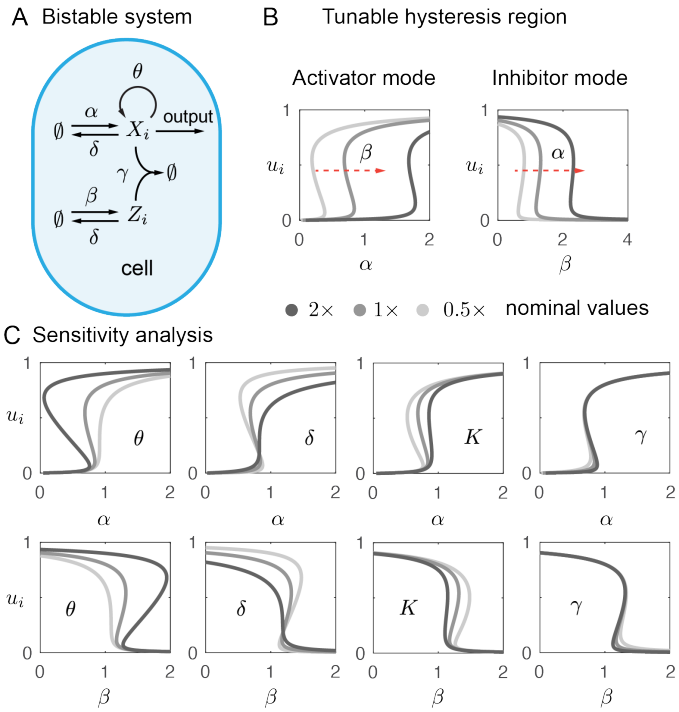

Fig. 3. **Tunable hysteresis enabled by molecular sequestration in a single bistable switch** Panel A illustrates the circuit design of a positive feedback loop coupled to a molecular sequestration mechanism. Panel B shows tunable input-output maps with varying α and β. Panel C demonstrates the effect of parameters on the input-output map. We use $K = 0.2$ for a better illustration in these sensitivity analysis plots.

TABLE I
Simulation Parameters.

Parameter	Description	Value	Other studies
$\alpha, \theta, \rho, \beta$ ($\mu M \cdot$ hr^{-1})	Production	1	$0.1 - 100$ [22], [23]
γ (μM^{-1} hr^{-1})	Sequestration	500	$36 - 3600$ [24], [25]
K (μM)	Dissociation	0.1	$10^{-5} - 1$ [26], [27]
δ, ϕ (hr^{-1})	Degradation	1	$0.36 - 3.6$ [28]

in Table I. We plot the steady state input-output maps in Fig. 3B for both activator mode (u_i versus α) and inhibitor mode (u_i versus β). Both maps show hysteresis, indicating two stable equilibria (ON and OFF states) and one unstable equilibrium (intermediate state).

When the bistable switch is applied as an ultrasensitive controller in the closed loop, the equilibrium should lie in the ultrasensitive regime, which is determined by the hysteresis threshold. Therefore, tuning the threshold can set the reference of the closed-loop output. To explore if the hysteresis is tunable, we change parameter values of β in the activator mode and α in the inhibitor mode by two folds, and generate more input-output maps in Fig. 3B. We observe that both parameters are able to change the hysteresis threshold in a large regime.

Next, we look for conditions on all parameters that ensure the bistability of this circuit analytically, and examine

how parameters affect hysteresis properties with sensitivity analysis.

B. Hysteresis Conditions And Sensitivity Analysis

First, to obtain hysteresis, there should be three distinct equilibrium in the steady state solution of equations (2)-(3). Since the variables represent concentrations of species, the solutions should be positive and real numbers.

We assume the sequestration between X_i and Z_i is fast [29], i.e., $\gamma \gg \frac{\alpha}{K^2}$. The analytical solutions can be approximated to find simple parameter conditions to admit three real roots (see Appendix A):

$$L_1 < \frac{\beta-\alpha}{\delta K} \quad \text{or} \quad \frac{\beta-\alpha}{\delta K} < U_1, \tag{5}$$

where

$$\begin{aligned} L_1 &= \frac{\theta}{\delta K} - \frac{\delta}{\gamma K} + 1 + 2\sqrt{\frac{\theta}{\delta K} - \frac{\theta}{\gamma K^2} - \frac{2\delta}{\gamma K}}, \\ U_1 &= \frac{\theta}{\delta K} - \frac{\delta}{\gamma K} + 1 - 2\sqrt{\frac{\theta}{\delta K} - \frac{\theta}{\gamma K^2} - \frac{2\delta}{\gamma K}}. \end{aligned}$$

We use Descarter's rule of sign to count the number of positive real solutions to admit three positive solutions (see Appendix A), which results in the following conditions:

$$L_2 < \frac{\beta-\alpha}{\delta K} < U_2, \tag{6}$$

where

$$L_2 = \frac{\theta}{\gamma K^2} + \frac{\delta}{\gamma K}, \quad \text{and} \quad U_2 = \frac{\theta}{\delta K} - \frac{\delta}{\gamma K} - 1.$$

The conditions to admit three distinct roots that are real and positive are set by the intersection of conditions (33) and (34). Note that $U_2 < L_1$, then the conditions become

$$L = L_2 < \frac{\beta-\alpha}{\delta K} < U = \min(U_1, U_2), \tag{7}$$

which can also be written as

$$\alpha + \delta KL < \beta < \alpha + \delta KU. \tag{8}$$

Equation (8) is a necessary condition for hysteresis. We first consider the inhibitor mode (u_i versus β). Equation (8) determines the β regime that can generate three equilibrium solutions, which is the necessary bistability region. Given a fixed α, boundaries of the bistability region are set by δKL and δKU. We notice that L and U do not depend on α. It means that varying α only switches the the hysteresis threshold linearly without changing the left and right boundaries. This observation is consistent with input-output maps under different α values shown in Fig. 3B, right panel.

For the activator mode (u_i versus α), we can rewrite equation (8) as

$$\beta - \delta KU < \alpha < \beta - \delta KL. \tag{9}$$

Similarly, the bistability region boundaries are set by δKU and δKL, and are not dependent on β. When varying β, only the hysteresis threshold is changed linearly, as shown in Fig. 3B, left panel.

Then we can inspect how parameters affect the bistability region by analyzing the sensitivity of boundaries δKL and δKU to parameters. For example, the sensitivity of δKL to parameter θ is defined as $\frac{\partial}{\partial\theta}(\delta KL) = \frac{\delta}{\gamma K}$. Similarly, we find sensitivity for other parameters: $\frac{\partial}{\partial\delta}(\delta KL) = \frac{\theta}{\gamma K} + 2\frac{\delta}{\gamma}$, $\frac{\partial}{\partial K}(\delta KL) = -\frac{\theta\delta}{\gamma K^2}$ and $\frac{\partial}{\partial\gamma}(\delta KL) = -\frac{\theta\delta}{\gamma^2 K} - \frac{\delta^2}{\gamma^2}$.

We focus on the inhibitor mode (u_i versus β) as an example of the analysis. We assume the sequestration rate is fast, where $\gamma \gg \theta/K^2, \delta/K$, then δKL becomes insensitive to parameters $\theta, \delta, K, \gamma$ since the sequestration rate γ is in the denominator of its sensitivity to all these parameters. It suggests that when we vary parameters θ, δ, K or γ, the left boundary of the bistability region will not present a large change, as also shown in Fig. 3C second row. On the other hand, the right boundary increases significantly with a larger θ and a smaller δ or K, according to the sensitivity analysis of δKU to these parameters. Similar conclusions can be drawn for the activator mode, which are consistent with input-output maps shown in Fig. 3C first row.

C. Local Stability Conditions

Next, we study the local stability criteria of equilibrium to ensure there are two stable and one unstable solutions. We proceed to find the linearization of the system (2)-(3) and the Jacobian matrix J is derived as:

$$J = \begin{bmatrix} -\delta - \gamma\bar{z}_i + \theta f_i & -\gamma\bar{x}_i \\ -\gamma\bar{z}_i & -\delta - \gamma\bar{x}_i \end{bmatrix}, \tag{10}$$

where $f_i = \frac{K}{(\bar{x}_i+K)^2}$. $\bar{x}_i$ and $\bar{z}_i$ are the equilibrium. By assessing the sign of the real part of eigenvalues, we find the local stability is guaranteed when

$$\delta^2 + \delta\gamma(\bar{x}_i + \bar{z}_i) > \theta(\gamma\bar{x}_i + \delta)f_i. \tag{11}$$

and local instability requires

$$\delta^2 + \delta\gamma(\bar{x}_i + \bar{z}_i) < \theta(\gamma\bar{x}_i + \delta)f_i. \tag{12}$$

In summary, hysteresis conditions and local stability conditions determine required parameter regimes for a bistable switch.

IV. Ultrasensitivity Emerges From Bistable Switches At Population Level

Now we evaluate the bistable switch circuit in a population-level setting, as shown in Fig. 4A. The population is considered as a collection of individual cells, where each cell has a bistable switch with the same input. They also generate an overall output $\hat{U}$. Therefore, bistable switches in parallel form the population level controller.

A. Multiple Switches In Parallel

We expand the model to include n cells with bistable switch circuits. The dynamics of all cells are

$$\dot{x}_i = \alpha + \theta\frac{x_i}{x_i + K} - \delta x_i - \gamma x_i z_i \tag{13}$$

$$\dot{z}_i = \beta - \delta z_i - \gamma x_i z_i. \tag{14}$$

for $i = 1 : n$. Since the population level controller generates an actuation to the population level dynamics through the

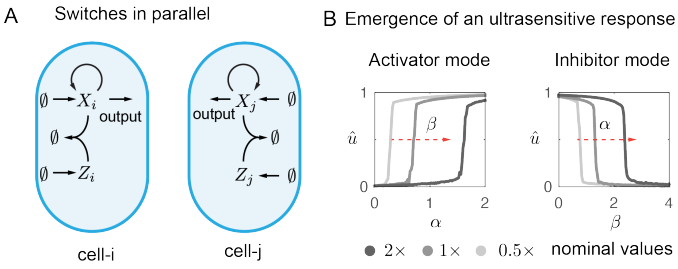

Fig. 4. **Multiple bistable switches in parallel** Panel A is a schematic figure of parallel bistable switches that represents a population of multiple cells. Panel B shows the population level steady state input-output mapping of multiple switches. We simulated for $n = 100$ cells.

overall activation in $\hat{Y}$ production by X_i in all cells, we define the total output of multiple bistable switches $\hat{U}$ as

$$\hat{u} = \sum_{i=1}^{n} u_i(x_i) = \sum_{i=1}^{n} \frac{x_i}{x_i + K}. \quad (15)$$

Again, we consider α and β are inputs to all bistable switches. Then we evaluate the steady state input-output maps: $\hat{u}$ versus α for the activator mode and $\hat{u}$ versus β for the inhibitor mode, by numerical simulations. As shown in Fig. 4B, the population level input-output map exhibits a graded increase or decrease along with the varying parameters. In contrast to a single bistable switch, multiple switches in parallel reach stable equilibrium in the ultrasensitive regime. Meanwhile, the thresholds of the graded maps are tunable in a large regime with changing parameters β and α.

B. Graded Output At Population Level

Multiple switches exhibit emergent properties in the input-output map. As shown in Fig. 4B, the total output has a graded response to the input, and all outputs admit stable equilibrium.

Recall that a single bistable switch only exhibits two stable states, ON and OFF states, and the intermediate state is unstable. The output of multiple switches is the sum of all single switch's states. Whenever a single bistable switch changes its state, the total output admits a new stable equilibrium. Since the numbers of single switches in ON states and OFF states are no longer restricted, the total output can reach a larger range of stable equilibrium. Therefore, in a population that consists of millions of cells, the extreme large number of bistable switches in parallel enables a smooth and graded response with stable outputs.

C. Emergent Ultrasensitivity At Population Level

Multiple switches also generate an ultrasensitivity input-output map at population level. The ultrasensitivity emerges from the sharp transition in single switches. To better understand how transition rates between ON and OFF states effect the ultrasensitive response, we consider a simple population level model of multiple switches:

$$\dot{n}_{on} = -f_+(\beta)n_{on} + f_-(\beta)n_{off} \quad (16)$$
$$\dot{n}_{off} = -f_-(\beta)n_{off} + f_+(\beta)n_{on} \quad (17)$$
$$n = n_{on} + n_{off}. \quad (18)$$

Variables n_{on} and n_{off} are total numbers of cells that exhibit ON and OFF states, and f_+ and f_- are transition rates from ON to OFF and vice versa. Here we focus on the inhibitor mode given a fixed α, so the transition rates depend on the input β. At steady state, we have

$$\overline{n}_{on} = \frac{f_-(\beta)}{f_+(\beta) + f_-(\beta)} \cdot n := r_{on}(\beta) \cdot n \quad (19)$$
$$\overline{n}_{off} = \frac{f_+(\beta)}{f_+(\beta) + f_-(\beta)} \cdot n := r_{off}(\beta) \cdot n. \quad (20)$$

Variables $r_{on}(\beta), r_{off}(\beta)$ are defined as population ratios of ON and OFF cells at steady state.

For simplicity, we assume a bistable switch at ON state generates an output U_{on}, and at OFF state it generates an output U_{off}. As defined in equation (4), the output of a single bistable switch depends on X_i concentration. Since the concentration of X_i is determined by input β in the inhibitor mode, we use $u_{on}(\beta)$ and $u_{off}(\beta)$ to represent the output values of ON state and OFF state switches in cells. According to equation (15) and equations (19)-(20), we can derive the population level output $\hat{U}$ at steady state as

$$\hat{u} = \overline{n}_{on}u_{on}(\beta) + \overline{n}_{off}u_{off}(\beta) \quad (21)$$
$$= \frac{f_-(\beta)u_{on}(\beta) + f_+(\beta)u_{off}(\beta)}{f_+(\beta) + f_-(\beta)} \cdot n. \quad (22)$$

It shows that the population level output $\hat{U}$ of bistable switches not only depends on the single cell level output, but also transition rates between states. We can find out in Fig. 3B, right panel, that the outputs at either ON state or OFF state are not very sensible to β and have rather flat curves compared to the intermediate transition. Meanwhile, transition rates $f_-(\beta), f_+(\beta)$ can be very sensitive to β in bistable switches. The population level input-output response becomes ultrasensitive because of sensitive transition rates.

We can also rewrite equation (22) with population ratios r_{on} and r_{off}:

$$\hat{u} = (r_{on}(\beta)u_{on}(\beta) + r_{off}(\beta)u_{off}(\beta)) \cdot n. \quad (23)$$

If we assume OFF state generates a very small output, i.e., $0 \approx u_{off} \ll u_{on}$, we can obtain

$$\hat{u} \approx r_{on}(\beta)u_{on}(\beta) \cdot n. \quad (24)$$

It implies an ultrasensitive controller can be achieved by sharp population ratio changes. In other words, if $r_{on}(\beta)$ is ultrasensitive to β, the output $\hat{u}$ becomes ultrasensitive, which only appears at population level. Such emergent properties suggest that bistable switch circuits can be used for ultrasensitive control at population level without requiring large productions in single cells.

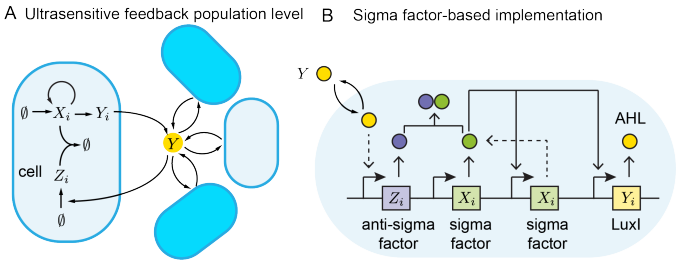

Fig. 5. **Closed-loop system with ultrasensitive feedback control** Panel A is the full circuit design with bistable switches and quorum sensing across the population. Panel B illustrates a synthetic circuit implementation using sigma and anti-sigma factors and quorum sensing molecules AHL.

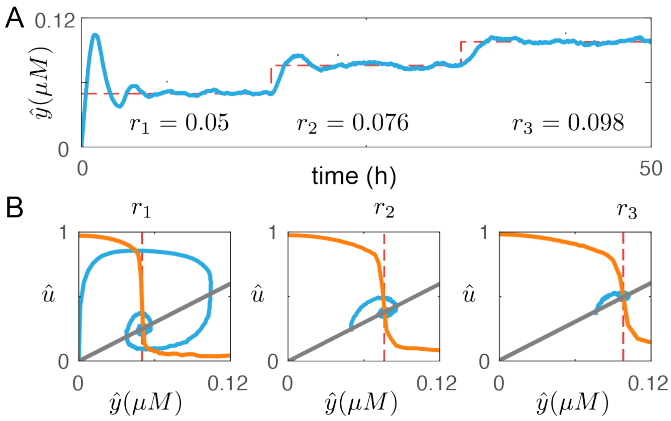

Fig. 6. **Robust tracking of references** Panel A shows the tracking of three different references in the closed-loop system. Panel B illustrates that tracking trajectories (blue line) converge towards the equilibrium determined by the intersection of the controller's input-output map (orange line) and the process's (gray line) input-output map.

V. Quorum Sensing Coordinates Bistable Switches In The Closed Loop

Finally, we apply bistable switch circuits as an ultrasensitive controller in the closed loop to control population level expressions. We use a quorum sensing system to link the population level process and controller. Quorum sensing signals can coordinate cells' state switching behaviors according to the error between the population output and the reference.

For simplicity, we consider the desired population output is the concentration of the quorum sensing signal. As shown in Fig. 5A, we adopt the inhibitor mode and link the output $\hat{Y}$ to the activation of Z_i, forming a negative feedback loop. A synthetic circuit implementation is also proposed in Fig. 5B. We suggest that a sigma factor activates itself and an enzyme LuxI that catalyzes the synthesis of a quorum sensing signaling molecule AHL. The signaling molecule diffuses across cell membranes and activates an anti-sigma factor that can sequester the sigma factor and form an inactive complex. There is another inducible production of the sigma factor, which can be used to set references by external inducers.

We assume the AHL concentration is proportional to the enzyme LuxI. Assuming AHL reaches quasi-steady state with fast diffusion, we do not specify the intracellular and extracellular concentrations. We also assume AHL activates anti-sigma factor following a Hill-type kinetics. Then we write down the model of the closed loop of n cells:

$$\dot{x}_i = \alpha + \theta \frac{x_i}{x_i + K} - \delta x_i - \gamma x_i z_i \tag{25}$$

$$\dot{z}_i = \beta \frac{y^2}{y^2 + K_y^2} - \delta z_i - \gamma x_i z_i \tag{26}$$

$$\dot{\hat{y}} = \rho \sum_{i=1}^{n} \frac{x_i}{x_i + K} - \phi \hat{y}, \tag{27}$$

for $i = 1 : n$. Equation (27) describes the dynamics of the total expression, which is the population level process. According to the definition of $\hat{u}$ in equation (15), we can also derive the steady state input-output map of the population level process:

$$\hat{y} = \frac{\rho}{\phi} \hat{u}. \tag{28}$$

In the closed loop, the population level controller takes $\hat{Y}$ as the input, since $\hat{Y}$ activates Z_i's production. We can numerically compute for the input-output map of the controller ($\hat{u}$ versus $\hat{y}$) by replacing β with $\beta \frac{y^2}{y^2+K_y^2}$ in the previous result of input-output map ($\hat{u}$ versus β). Then the intersection of input-output maps should determine the steady state equilibrium of the closed-loop system.

A. Reference Tracking Performance

We first test if the population level output $\hat{Y}$ tracks different references. The references are set by the external induction, represented by parameter α in the model. We set three different references by increasing α.

We run a stochastic simulation of $n = 100$ cells in parallel and plot the time trajectory in Fig. 6A. The population output $\hat{Y}$ (blue line) closely tracks each reference (dashed red line). Fig. 6B shows input-output maps of the population level process and controller under each corresponding reference. The process (gray line) shows a linear input-output map, as derived in equation (28), and the input-output map of the controller (orange line) exhibits ultrasensitivity. The threshold of the controller's input-output map is moved towards the right when α is set with a larger value. We find that the closed-loop trajectory of $\hat{Y}$ (blue line) indeed converges to the intersection of input-output maps of the process and the controller. The equilibrium determined by the intersection falls in the neighborhood of the threshold, which is consistent with the previous analysis of the controller.

B. Disturbance Rejection Performance

Next, we test if the closed-loop system can adapt to disturbances in the process dynamics via the ultrasensitive controller. We consider step disturbances that perturb the production rate ρ and degradation and dilution rate ϕ of $\hat{Y}$.

In Fig. 7A, the time trajectory shows the population level output can adapt to disturbances with very small errors. It is more clear in Fig. 7B that the ultrasensitive feedback ensures the output $\hat{Y}$ to converge to the same concentration even with large changes in the process due to disturbances. The gray lines in the middle and right panels illustrate how the process

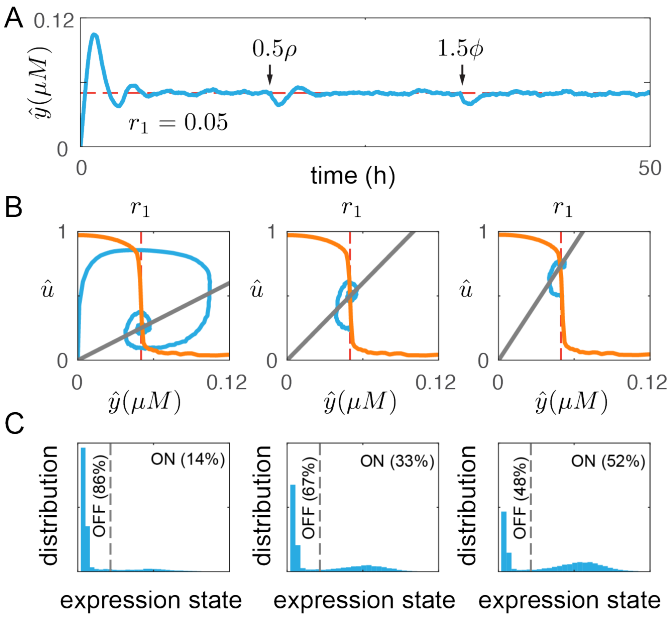

Fig. 7. **Robust adaptation to disturbances in the process dynamics** Panel A shows the adaptation of the closed-loop system when the process undergoes disturbances such as a decreased production rate ρ and a increased of degradation and dilution rate ϕ. Panel B shows input-output mappings of the controller and the process. All intersections are within the ultrasensitive regime, so the trajectories all converge to the same output determined by the threshold. Panel C illustrates the adaptation is achieved at population level by changing the ratio of cells in ON and OFF states.

is disturbed with a smaller ρ and a larger ϕ, compared to the left panel. Moreover, if we look at the expression state distribution for each condition in Fig. 7C, more cells switch to ON state to adapt to the disturbance of a lower production or higher degradation and dilution, indicating the adjustment in heterogeneous population ratios fulfills the ultrasensitive feedback at population level, as demonstrated in equation (24).

In summary, with the bistable switch circuit and quorum sensing system, the population level expression robustly tracks references that are set externally and adapts to disturbances in the process dynamics. In this circuit, we consider the quorum sensing signal concentration as the target population expression. More generally, any species of interest can be controlled by having the target gene and quorum sensing signal production both activated by the controller. In that case, the quorum sensing signal can be approximated as a proportional measurement of the target expression. In addition, we can use the activator mode of the controller for more diverse implementations. Instead of having X_i activates Y_i and $\hat{Y}$ activates Z_i, X_i can be a repressor of Y_i and $\hat{Y}$ can be designed to activate X_i to close the negative feedback loop. In the activator mode, external induction in Z_i production can set the reference, which refers to β in the model.

VI. Discussion

In this paper, we present a design principle of ultrasensitive feedback control based on bistable switch to realize robust and tunable population expressions. The controller includes a positive loop with sequestration to generate bistability in single cell expressions. The quorum sensing system closes the loop and ensures stable and robust population level dynamics.

In theory, we are able to predict the tunability in population level outputs by characterizing single cell level hysteresis. The analytical results set criteria of parameters and constraints on corresponding regulation network structures to achieve bistability. Besides the bistable switch presented in this paper, other circuits that have ultrasensitive responses such as toggle switches, phosphorylation cycles, recombinase protein switches can also be rewired with quorum sensing systems to form an ultrasensitve feedback controller at population level.

The key design strategy of ultrasenstive controllers at population level proposed in this paper is state switching. The required ultrasensitive response of the controller is fulfilled by sharp state switching that leads to a significant population ratio change between heterogeneous phenotypes. We demonstrate such behaviors with numerical simulations, yet more work need to be done in theory to understand what conditions guarantee the ultrasensitive response at population level. Here, we want to emphasize the potential of heterogeneity in population level design. Instead of inducing large productions in all single cells, state switching in heterogeneous populations can divide the labor and relieve burden in cells. We believe the heterogeneity can be harnessed in synthetic circuits to achieve more robust functionalities to environmental disturbances as well as to increase population's resilience to stress and mutations.

In general, design principles at population level are needed besides single cell level designs, since population level behaviors can be more complex than single cells. Cell-cell communication, for example quorum sensing systems presented in this paper, can be used to coordinate cell behaviors, thus it has a great potential in population control problems. Recent studies have applied cell-cell communication to control bacterial population densities [30], [31]. It is also proposed in theory that cell-cell communication can improve population level robustness in general through an intercellular layer of feedback [32]. By engineering cell-cell communications, we expect more complicated functionalities to be achieved in microbial consortia even with multiple cell types.

VII. Acknowledgments

The authors would like to thank Fangzhou Xiao and Ronghui Zhu for their insightful discussions. The authors X. R is sponsored by the Defense Advanced Research Projects Agency (Agreement HR0011-17-2-0008). EF is sponsored by NSF/BBSRC award 2020039. The content of the information does not necessarily reflect the position or the policy of the Government, and no official endorsement should be inferred.

APPENDIX

A. Derivation for bistability conditions

We can find the steady state expression by making all equation (2)-(3) equal to zero. This results in

$$\bar{z}_i = \frac{\alpha^* - \delta\bar{x}_i}{\gamma\bar{x}_i} = \frac{\beta}{\gamma\bar{x}_i + \delta} \tag{29}$$

where $\alpha^* = \alpha + \theta\frac{x_i}{x_i+K}$. This results in a third order polynomial

$$P(\frac{\bar{x}_i}{K}) = (\frac{\bar{x}_i}{K})^3 + B(\frac{\bar{x}_i}{K})^2 + C(\frac{\bar{x}_i}{K}) + D = 0, \tag{30}$$

where $B = \frac{\beta-\alpha-\theta}{\delta K} + 1 + \frac{\delta}{\gamma K}$, $C = \frac{\beta-\alpha}{\delta K} - \frac{\theta+\alpha}{\gamma K^2} - \frac{\delta}{\gamma K}$, and $D = -\frac{\alpha}{\gamma K^2}$.

We use the general solution of a third order polynomial, $P(\bar{x}_i/K)$, to find conditions to admit three real solutions. This leads to

$$\Delta = 18BCD - 4B^3D + B^2C^2 - 4C^3 - 27D^2 > 0 \tag{31}$$

On the other hand, when $\Delta < 0$, $P(\bar{x}_i/K)$ can only admit a single real solution.

We consider the case when $\gamma \gg \frac{\alpha}{K^2}$, making $D \approx 0$. Then we can simplify the condition on the number of real solutions as

$$\Delta \approx C^2(B^2 - 4C) > 0. \tag{32}$$

This leads to

$$L_1 < \frac{\beta-\alpha}{\delta K} \quad \text{or} \quad \frac{\beta-\alpha}{\delta K} < U_1, \tag{33}$$

where

$$\begin{aligned} L_1 &= \frac{\theta}{\delta K} - \frac{\delta}{\gamma K} + 1 + 2\sqrt{\frac{\theta}{\delta K} - \frac{\theta}{\gamma K^2} - \frac{2\delta}{\gamma K}}, \\ U_1 &= \frac{\theta}{\delta K} - \frac{\delta}{\gamma K} + 1 - 2\sqrt{\frac{\theta}{\delta K} - \frac{\theta}{\gamma K^2} - \frac{2\delta}{\gamma K}}. \end{aligned}$$

This condition does not tell us about the sign of the three real solutions. Next, we use Descarter's rule of sign of $P(\bar{x}_i/K)$ to admit three positive real solution. We need three sign changes in $(1, B, C, D)$. Thus, we require $B < 0$, $C > 0$ and $D < 0$, resulting in

$$L_2 < \frac{\beta-\alpha}{\delta K} < U_2, \tag{34}$$

where

$$L_2 = \frac{\theta}{\gamma K^2} + \frac{\delta}{\gamma K}, \quad \text{and} \quad U_2 = \frac{\theta}{\delta K} - \frac{\delta}{\gamma K} - 1.$$

REFERENCES

[1] W. Sabra, D. Dietz, D. Tjahjasari, and A.-P. Zeng, "Biosystems analysis and engineering of microbial consortia for industrial biotechnology," *Engineering in Life Sciences*, vol. 10, no. 5, pp. 407–421, 2010.

[2] H. Alper and G. Stephanopoulos, "Engineering for biofuels: exploiting innate microbial capacity or importing biosynthetic potential?" *Nature Reviews Microbiology*, vol. 7, no. 10, pp. 715–723, 2009.

[3] J. Claesen and M. A. Fischbach, "Synthetic microbes as drug delivery systems," *ACS synthetic biology*, vol. 4, no. 4, pp. 358–364, 2015.

[4] J. Stelling, U. Sauer, Z. Szallasi, F. J. Doyle III, and J. Doyle, "Robustness of cellular functions," *Cell*, vol. 118, no. 6, pp. 675–685, 2004.

[5] N. Venayak, N. Anesiadis, W. R. Cluett, and R. Mahadevan, "Engineering metabolism through dynamic control," *Current opinion in biotechnology*, vol. 34, pp. 142–152, 2015.

[6] M. R. Charbonneau, V. M. Isabella, N. Li, and C. B. Kurtz, "Developing a new class of engineered live bacterial therapeutics to treat human diseases," *Nature Communications*, vol. 11, no. 1, pp. 1–11, 2020.

[7] T.-M. Yi, Y. Huang, M. I. Simon, and J. Doyle, "Robust perfect adaptation in bacterial chemotaxis through integral feedback control," *Proceedings of the National Academy of Sciences*, vol. 97, no. 9, pp. 4649–4653, 2000.

[8] W. Ma, A. Trusina, H. El-Samad, W. A. Lim, and C. Tang, "Defining network topologies that can achieve biochemical adaptation," *Cell*, vol. 138, no. 4, pp. 760–773, 2009.

[9] D. Muzzey, C. A. Gómez-Uribe, J. T. Mettetal, and A. van Oudenaarden, "A systems-level analysis of perfect adaptation in yeast osmoregulation," *Cell*, vol. 138, no. 1, pp. 160–171, 2009.

[10] S. K. Aoki, G. Lillacci, A. Gupta, A. Baumschlager, D. Schweingruber, and M. Khammash, "A universal biomolecular integral feedback controller for robust perfect adaptation," *Nature*, vol. 570, no. 7762, pp. 533–537, 2019.

[11] C. C. Samaniego and E. Franco, "An ultrasensitive biomolecular network for robust feedback control," *IFAC-PapersOnLine*, vol. 50, no. 1, pp. 10 950–10 956, 2017.

[12] ——, "Ultrasensitive molecular controllers for quasi-integral feedback," *bioRxiv*, 2018.

[13] D. Del Vecchio, A. J. Dy, and Y. Qian, "Control theory meets synthetic biology," *Journal of The Royal Society Interface*, vol. 13, no. 120, p. 20160380, 2016.

[14] M. Kaern, T. C. Elston, W. J. Blake, and J. J. Collins, "Stochasticity in gene expression: from theories to phenotypes," *Nature Reviews Genetics*, vol. 6, no. 6, pp. 451–464, 2005.

[15] N. Q. Balaban, J. Merrin, R. Chait, L. Kowalik, and S. Leibler, "Bacterial persistence as a phenotypic switch," *Science*, vol. 305, no. 5690, pp. 1622–1625, 2004.

[16] M. Thattai and A. Van Oudenaarden, "Stochastic gene expression in fluctuating environments," *Genetics*, vol. 167, no. 1, pp. 523–530, 2004.

[17] S. A. West and G. A. Cooper, "Division of labour in microorganisms: an evolutionary perspective," *Nature Reviews Microbiology*, vol. 14, no. 11, pp. 716–723, 2016.

[18] N. Olsman, A.-A. Baetica, F. Xiao, Y. P. Leong, R. M. Murray, and J. C. Doyle, "Hard limits and performance tradeoffs in a class of antithetic integral feedback networks," *Cell systems*, vol. 9, no. 1, pp. 49–63, 2019.

[19] Y. Qian and D. Del Vecchio, "Realizing 'integral control'in living cells: how to overcome leaky integration due to dilution?" *Journal of The Royal Society Interface*, vol. 15, no. 139, p. 20170902, 2018.

[20] S. Hooshangi and W. E. Bentley, "From unicellular properties to multicellular behavior: bacteria quorum sensing circuitry and applications," *Current Opinion in Biotechnology*, vol. 19, no. 6, pp. 550–555, 2008.

[21] D. Chen and A. P. Arkin, "Sequestration-based bistability enables tuning of the switching boundaries and design of a latch," *Molecular systems biology*, vol. 8, no. 1, p. 620, 2012.

[22] Y. Qian, H.-H. Huang, J. I. Jiménez, and D. Del Vecchio, "Resource competition shapes the response of genetic circuits," *ACS synthetic biology*, vol. 6, no. 7, pp. 1263–1272, 2017.

[23] S. Basu, Y. Gerchman, C. H. Collins, F. H. Arnold, and R. Weiss, "A synthetic multicellular system for programmed pattern formation," *Nature*, vol. 434, no. 7037, pp. 1130–1134, 2005.

[24] J. Kim, K. S. White, and E. Winfree, "Construction of an in vitro bistable circuit from synthetic transcriptional switches," *Molecular systems biology*, vol. 2, no. 1, p. 68, 2006.

[25] D. Y. Zhang, A. J. Turberfield, B. Yurke, and E. Winfree, "Engineering entropy-driven reactions and networks catalyzed by dna," *Science*, vol. 318, no. 5853, pp. 1121–1125, 2007.

[26] M. Liu, G. Gupte, S. Roy, R. P. Bandwar, S. S. Patel, and S. Garges, "Kinetics of transcription initiation at lacp1 multiple roles of cyclic amp receptor protein," *Journal of Biological Chemistry*, vol. 278, no. 41, pp. 39 755–39 761, 2003.

[27] R. Milo, P. Jorgensen, U. Moran, G. Weber, and M. Springer, "Bion-

umbers—the database of key numbers in molecular and cell biology," *Nucleic acids research*, vol. 38, no. suppl_1, pp. D750–D753, 2010.
[28] J. Kim, I. Khetarpal, S. Sen, and R. M. Murray, "Synthetic circuit for exact adaptation and fold-change detection," *Nucleic acids research*, vol. 42, no. 9, pp. 6078–6089, 2014.
[29] N. E. Buchler and F. R. Cross, "Protein sequestration generates a flexible ultrasensitive response in a genetic network," *Molecular systems biology*, vol. 5, no. 1, p. 272, 2009.
[30] L. You, R. S. Cox, R. Weiss, and F. H. Arnold, "Programmed population control by cell–cell communication and regulated killing," *Nature*, vol. 428, no. 6985, pp. 868–871, 2004.
[31] X. Ren, A.-A. Baetica, A. Swaminathan, and R. M. Murray, "Population regulation in microbial consortia using dual feedback control," in *2017 IEEE 56th Annual Conference on Decision and Control (CDC)*. IEEE, 2017, pp. 5341–5347.
[32] X. Ren and R. M. Murray, "Layered feedback control improves robust functionality across heterogeneous cell populations," *bioRxiv*, 2020.